

# Identification of candidate genes simultaneously shared by adipogenesis and osteoblastogenesis from human mesenchymal stem cells

Xia Yi\* , Ping Wu , Yunyan Fan , Ying Gong, Jianyun Liu , Jianjun Xiong\* , Xiaoyuan Xu\* 

Jiangxi Provincial Key Laboratory of Systems Biomedicine, Jiujiang University, Jiujiang, China

## Abstract

**Introduction.** In osteoporosis field, it had been clinically well established a given relationship between bone formation and lipid accumulation. Although numerous molecules had been well documented for adipogenesis and osteoblastogenesis (adipo-osteoblastogenesis), the reciprocal transcriptional regulation still remains to be explored.

**Material and methods.** Here, we tried to identify the common candidate genes of adipocyte/osteoblastocyte differentiation at 3, 5, and 7 days using human mesenchymal stem cells (hMSCs) *via* RNA-Seq technique. By using RNA interference (RNAi), we further confirmed the function of candidate genes during adipo-osteoblastogenesis through Oil Red/Alizarin Red/alkaline phosphatase (ALPL) staining and qRT-PCR (quantitative real-time PCR).

**Results.** The identified 275 significantly differentially expressed genes (DEGs), especially with the down-regulated genes most prevalent and PI3K-AKT signaling pathway mostly enriched, were simultaneously shared by both differentiation events. Using lentiviral system, we further confirmed that *ANKRD1* (ankyrin repeat domain 1) promoted adipogenesis and inhibited osteoblastogenesis *via* RNA interference (RNAi), and *IGF1* (insulin like growth factor 1) simultaneously facilitated adipo-osteoblastogenesis on the base of gene expression of biomarkers and cellular phenotype property.

**Conclusion.** This study would provide the potential molecular switches to control the adipocyte/osteoblastocyte balance or hMSCs fate choices and clues to screen the study and therapy targets of metabolic bone disease osteoporosis. (*Folia Histochemica et Cytobiologica* 2022, Vol. 60, No. 2, 179–190)

**Keywords:** human mesenchymal stem cells; adipogenesis; osteoblastogenesis; *ANKRD1*; *IGF1*

## Introduction

Adipogenesis and osteoblastogenesis (adipo-osteoblastogenesis) from the multipotent human mesenchymal stem cells (hMSCs) were closely correlated with the events facilitating cell fate to one of adipocyte or osteoblastocyte while repressing the other [1]. Plasticity between adipocytes and osteoblastocytes sharing a common ancestor in adult bone marrow was important for the etiology of osteoporosis and other

bone metabolic diseases involving with an imbalance of the two cell lineages [2]. Affirmatively, it had been clinically well established that a decrease of bone volume was involved with osteoporosis accompanied by an increase of marrow adipose tissue [3].

In recent years, the study of hMSCs differentiation had received robust attention due to bone metabolic diseases. The balance of adipo-osteoblastogenesis from hMSCs was controlled by key genes [4–8], regulators [9–12], signaling pathways [13–15], circulating cytokines [16], and stimuli [17–19]. Of course, the quest for adipo-osteoblastogenic differentiation was also constantly elucidated in multipotent stem cells *via* transcriptomic technique [20–22]. However, the co-regulation of adipo-osteoblastogenesis from hMSCs still remained controversial evidence.

In this study, we carried out RNA deep sequencing to identify candidate genes simultaneously shared

\*Correspondence address: Xia Yi

Jiangxi Provincial Key Laboratory of Systems Biomedicine,  
Jiujiang University, 17 Lufeng Road, Jiujiang 332000, China  
e-mail: yixia@mail.ecust.edu.cn

Co-authors' e-mails:

Jianjun Xiong, jcyx\_xiongjianjun@jju.edu.cn;  
Xiaoyuan Xu, xiaoyuan.xu@vip.163.com

by adipo-osteoblastogenesis at 3, 5, and 7 days from hMSCs. Interestingly, 275 significant DEGs, especially with the down-regulated genes most prevalent, were identified as candidate genes for the two differentiation lineages. We further investigated the gene function of two candidate genes, *ANKRD1* and *IGF1*, during two differentiation events using a lentiviral system. This remarkable advance in the identification of candidate genes co-regulating adipo-osteoblastogenesis would provide the potential molecular switches to control the adipocyte/osteoblastocyte balance or hMSCs fate choices and clues to screen the key study and therapy factors of metabolic bone disease osteoporosis.

## Material and methods

**hMSCs isolation, culture, and differentiation.** Identified in our previous study [23], the hMSCs were isolated from a 21-year-old non-osteoporotic healthy male volunteer recruited by Affiliated Hospital of Jiujiang University, Jiujiang, China, following the protocols with slight modification [24–25]. Adipogenic differentiation assays were performed according to the documented method with slight modifications [26]. In a Model 3100 series Forma Series II Water Jacket CO<sub>2</sub> incubator (Thermo Fisher Scientific, Ohio, United States), the hMSCs were cultured in 5.0 mL hMSCs Basal Medium (Cyagen bioscience, Inc., Santa Clara, CA, USA) containing FBS (fetal bovine serum), L-glutamine, and penicillin-streptomycin in 25 cm<sup>2</sup> flasks (Corning Incorporated, Corning, New York, NY, USA) at 37°C with 5% CO<sub>2</sub> and 95% humidity. Adipogenic differentiation process was inspired using adipogenic cocktails with 1.0 μM dexamethasone, 0.5 mM 3-isobutyl-1-methyl-xanthine, and 0.01 mg/mL insulin (Sigma, St. Louis, Mo, USA) in Gibco MEMα (Minimum Essential Medium Alpha) every three days after hMSCs were expanded to passage 6 with 80–90% of the final confluence (approximately at a density of 5.0 × 10<sup>4</sup> cells/cm<sup>2</sup>). The adipogenic potential was determined through staining assays of Oil Red O (Cyagen bioscience, Inc.) [27, 28].

For osteoblastogenic differentiations, passage 6 of the hMSCs were seeded at 10<sup>8</sup> cells/cm<sup>2</sup> and cultured to 70% confluence in hMSCs Basal Medium (Cyagen bioscience, Inc.), and then induced with osteoblastogenic differentiation medium supplemented with FBS, β-glycerophosphate, L-glutamine, ascorbic acid, dexamethasone, penicillin and streptomycin purchased from Sigma (St. Louis, MO, USA) every three days. Here, osteoblastogenic potential was determined *via* Alizarin Red staining and alkaline phosphatase (ALPL) staining and enzyme activity determination. Calcium-bound Alizarin Red for osteoblastocytes was eluted after incubated with 100 mM cetylpyridinium chloride for 1 h to quantify the matrix mineralization and measured at a wavelength of

570 nm [29]. For ALPL staining, osteoblastocytes in 6-well plate at 0, 3, 5, and 7 days were stained using the ALPL staining kit (Beijing ComWin Biotech Co., Ltd., Beijing, China) at room temperature for 10 min after fixed in cold ethanol for 10 min [30]. And then we captured the images under a microscope (IX73, Olympus, Tokyo, Japan). ALPL enzyme activity was determined using the ALPL assay kit (Nanjing Jiancheng Bioengineering Institute, Nanjing, China) after lysing osteoblastocytes using 1.0% Triton-X100 for 40 min on ice. The optical density value was measured at a wavelength of 520 nm.

**RNA sequencing and data analysis.** The freshly harvested cells of adipo-osteoblastogenesis were immediately used to isolate the total RNA using TRIzol reagent (Invitrogen, Carlsbad, CA, USA) following the manufacturer's instructions. The obtained RNA purified with the NucleoSpin RNA clean-up kit (Macherey-Nagel, Düren, Germany) was qualified using Bioanalyzer 2200 (Agilent Technologies, Santa Clara, CA, USA). Except for the centrifugation steps at 4°C, the other whole isolation procedure was carried out on ice under a vent. The total RNA was kept snap-frozen at –80°C for the downstream applications.

RNA-Seq assays were performed by Shanghai NovelBio Co., Ltd., China. The rRNA depletion library of RIN (RNA integrity number) > 6.0 was constructed using NEBNext® Ultra™ Directional RNA Library Prep kit according to the manufacturer's instructions. The whole transcriptome sequencing was performed on HiSeq™ Sequencer after filtering the adaptor sequences (reads with > 5% ambiguous bases) and low-quality reads (more than 20 percent of bases with qualities of < 20). HTSeq was used to calculate the gene count of mRNA [31]. DAVID (Database for Annotation, Visualization, and Integrated Discovery) and IPA (Ingenuity pathway analysis) were separately used to analyze gene ontology (GO) and KEGG pathway with *p*-value < 0.05. Here, differentially expressed genes (DEGs) were defined as the threshold of an absolute value of the log<sub>2</sub> ratio ≥ 2.0, and the significance threshold for the DEGs was set with log<sub>2</sub> ratio ≥ 2.0 and a false discovery rate (FDR) < 0.001.

**qRT-PCR.** Quantitative real-time PCR (qRT-PCR) on a 7500 Real Time PCR System (ABI, Foster City, CA, USA) was employed to determine the relative gene expression level. The oligonucleotide primers synthesized by Generay Biotech Co., Ltd (Shanghai, China) in this study were listed in Table 1. Approximately 2.0 μg of total RNA was converted to cDNA using the ReverTra Ace qPCR RT kit (Torobo, Osaka, Japan). With the SYBR Green Realtime PCR Master Mix (Torobo, Osaka, Japan), qRT-PCR was carried out at 94°C for 5 min, and 52°C for 34 sec, and final extension at 72°C with 30 cycles. The gene ACTB (actin beta) was used as the internal control [32]. All the assays were performed in triplicate.

**Table 1.** Oligonucleotide primers in this study

| Gene   | Product  | Primer                 |
|--------|--|------------------------|
| ACTB   | Actin beta   | CGAGGACTTTGATTGCACATTG |
|        |  | AGAGAAGTGGGGTGGCTTTTAG |
| ALPL   | Alkaline phosphatase, biomineralization associated | TTTCTCTGGGCAGGCAG      |
|        |  | GTTCCACGGAGGCTTCAG     |
| ANKRD1 | Ankyrin repeat domain 1                            | GCAAGGGAAGGCATGTAGGGAC |
|        |  | CTGGGGTAAAATAGCTGGCTT  |
| FABP4  | Fatty acid binding protein 4                       | GAGAGGATGATAAACTGGTGGT |
|        |  | GAATGTTGTAGAGTTCAATGCG |
| IGF1   | Insulin like growth factor 1                       | CCTCAGACAGGCATCGTG     |
|        |  | TGACTTGGCAGGCTTGAG     |
| LPL    | Lipoprotein lipase                                 | GGAAAACAGTCGATCAAGGG   |
|        |  | GGCACGATCATCTCTCTCAG   |
| PPARG  | Peroxisome proliferator activated receptor gamma   | TGCAAGGGTTTCTCCGG      |
|        |  | ATCCCCACTGCAAGGCAT     |
| RUNX2  | RUNX family transcription factor 2                 | GGACCTGTGCTTCTGCC      |
|        |  | TACTTGGTATACGGCCTTTAGA |
| SP7    | Sp7 transcription factor                           | TAGATGTGCTCTTTGGGG     |
|        |  | TAGAGAAAGCCTTCCCA      |

**Cell transfection.** ANKRD1 and IGF1 were inversely and differentially expressed during adipo-osteoblastogenesis, so we tentatively selected ANKRD1 and IGF1 to investigate gene function during adipo-osteoblastogenesis through RNA interference (RNAi) assays. The sequences, 5' — caGAATGGAACCAAAGCAATA — 3' for ANKRD1 (NM\_014391), 5' — GTCCTCCTCGCATCTCTCTCTA — 3' for IGF1 (NM\_00111283), and 5' — TTCTCGAACGTGTCACGT — 3' for the negative control, were synthesized commercially by Genechem Co., Ltd (Shanghai, China) separately to knock down ANKDRD and IGF1 and constructed in pGV493-GFP vector with to establish the expressing plasmid for RNAi following the standard subcloning procedures. Primers for the overexpression of ANKRD1 (NM\_014391) and IGF1 (NM\_00111283) could be obtained from our corresponding authors upon the reasonable request.

The experiments of cell transfection for ANKRD1-siRNA and IGF1-siRNA were performed at 20% confluence of hMSCs using HitransG Transfection Reagent P (Genechem Inc., Shanghai, China) according to the manufacturer's instruction.

With 20% confluence of the hMSCs passage 6, we performed cell transfection of ANKRD1-siRNA and IGF1-siRNA using HitransG Transfection Reagent P (Genechem Inc., Shanghai, China) according to the manufacturer's instruction.

**Statistical analysis.** Results express mean  $\pm$  SD. Depending on normality test data were analyzed by Student's *t*-test or the Mann-Whitney Rank Sum Test wherever appropriate (SigmaPlot software, version 14, SPSS, USA). *P* < 0.05 was set as significance level.

## Results

### *Adipo-osteoblastogenic differentiation*

The expanded hMSCs were separately induced towards adipo-osteoblastogenic differentiation. Adipogenic potential was measured *via* Oil Red O staining assays (Fig. 1). No lipid droplet was accumulated at 0 day (Fig. 1a). Few lipid droplets were visible at 3 days after adding adipogenic cocktails (Fig. 1b). The number and size of the lipid droplets continuously increased from 5 to 7 days during adipogenesis (Fig. 1c, d). Osteoblastogenic differentiation was demonstrated *via* Alizarin Red staining of calcified bone matrix (Fig. 1e–h). Besides the abnormal osteoblastocytes with a more rounded and cobblestone-like shape and less staining for increased secretion of mineralized bone matrix, we also obtained some clear signs of the increased ALPL activity *via* the quantification of the red derivative quinones (Fig. 1i–l) with cell cultivation time prolonged. It indicated that our hMSCs separately differentiated along adipo-osteoblastogenesis.

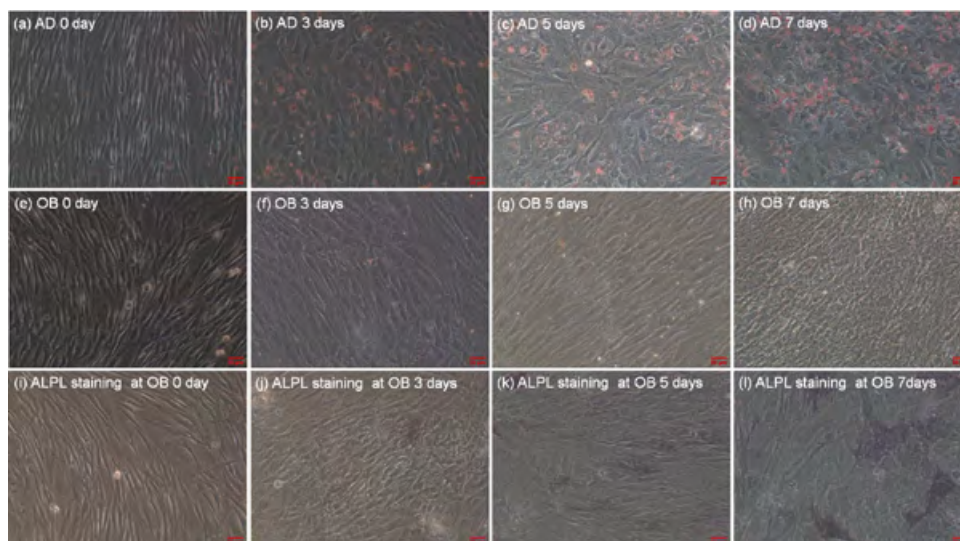


**Figure 1.** Adipo-osteoblastogenic potential of human mesenchymal stem cells (hMSCs) at 0 day, 3 days, 5 days, and 7 days. a-d, e-h, and i-l separately indicated Oil Red O staining, Alizarin Red staining, and ALPL (alkaline phosphatase, biomineralization associated) staining. Space bar: 20  $\mu\text{m}$ .

### **Transcriptional response during adipo-osteoblastogenesis**

Here, RNA-Seq technique was carried out to investigate the gene transcription of adipo-osteoblastogenesis from hMSCs. We identified 275 DEGs from an intersection calculation of three time points as candidate genes simultaneously shared by adipo-osteoblastogenesis (Fig. 2). There're 101 DEGs was separately up-regulated at 3, 5, and 7 days during adipogenesis, and 174 DEGs were down-regulated. 99, 101, and 99 DEGs were up-regulated at 3, 5, and 7 days during osteoblastogenesis, and 176, 174, and 176 DEGs were down-regulated. All in all, the down-regulated genes were most prevalent in both differentiation events. Interestingly, six DEGs, including ANKRD1 (ankyrin repeat domain 1), BPIFB4 (BPI fold containing family B member 4), DIRC3 (disrupted in renal carcinoma 3), IGF1 (insulin-like growth factor 1), PRR15 (proline-rich 15), and SCARA5 (scavenger receptor class A member 5), were of the entirely opposite expression profiling separately in response to two differentiation events, of which ANKRD1 and IGF1 were significantly differentially expressed, and thus suggested that the above six genes might participate in the two events in different regulation forms. GO analysis showed that 275 DEGs were mostly concerned with signal transduction, multicellular organismal development, and positive regulation of cell proliferation (Fig. 3). KEGG pathway analysis uncovered that PI3K-AKT signaling pathway was the most enriched pathway (Fig. 4).

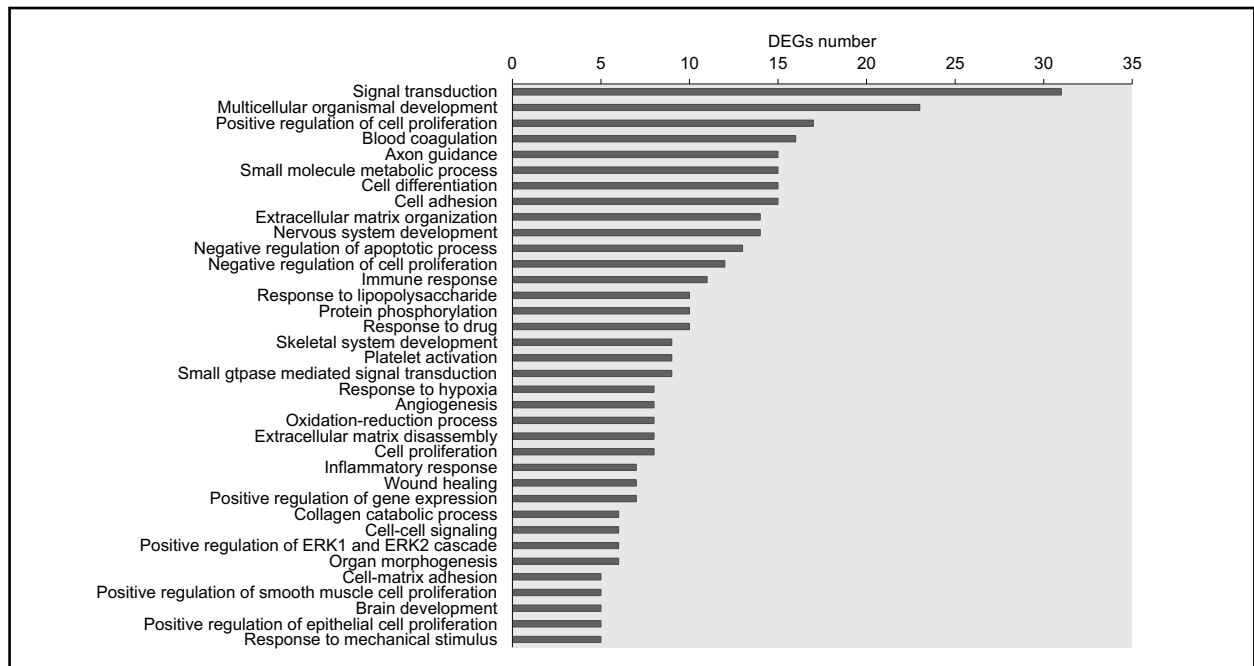
### **Validation studies of the selected candidate genes**

The two selected candidate genes, ANKRD1 and IGF1, were subjected to additional validation experiments. With the reporter gene GFP expressing, we confirmed that the hMSCs were successfully transfected separately with ANKRD1 and IGF1 overexpressed or knocked down using a lentiviral system (Fig. 5a, b).

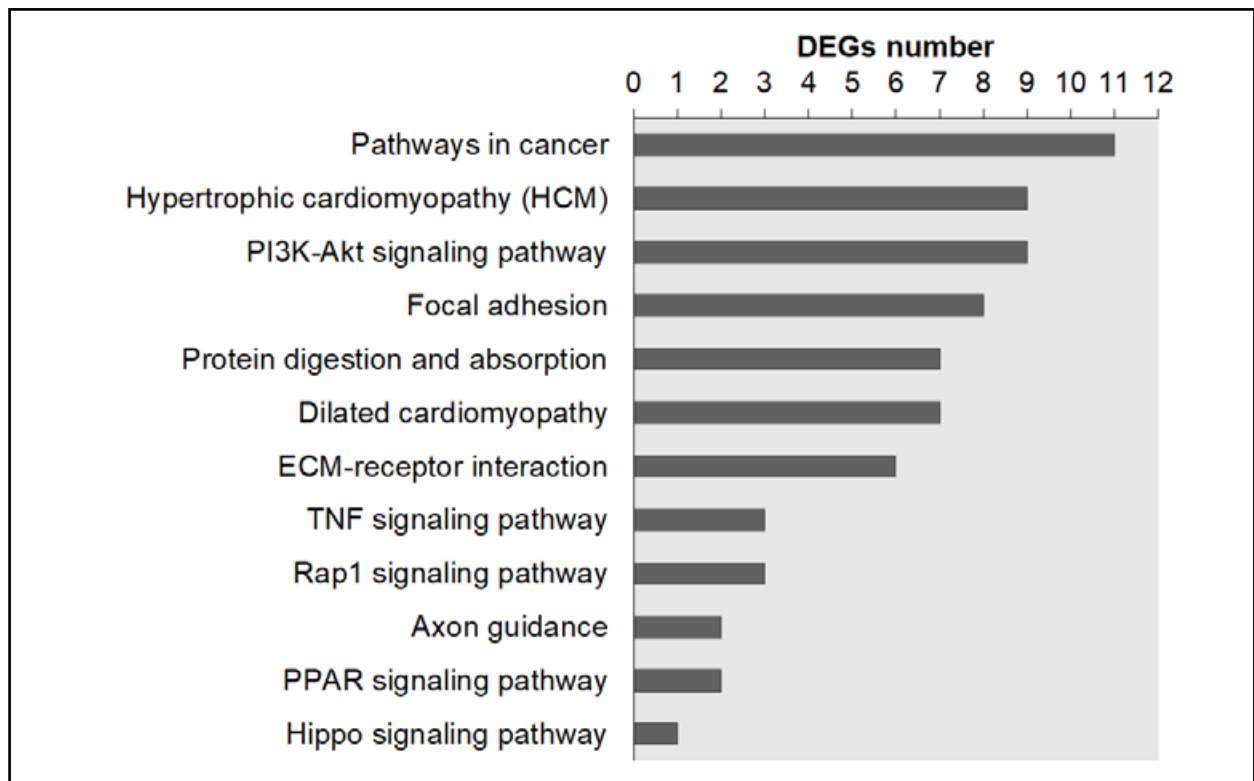
ANKRD1 was significantly differentially down-regulated by 13.55, 4.32, and 5.01 folds during adipogenesis and up-regulated by 4.96, 5.05, and 4.83 folds during osteoblastogenesis (Fig. 2). For adipogenesis, with ANKRD1 overexpressed *via* RNAi, the expression level of the adipogenic biomarkers was increased at the transcriptional and the translational levels at 3, 5, and 7 days (Fig. 5a-c). Compared with the negative control, lipid droplet accumulation was also increased (Fig. 5d). For osteoblastogenesis, ANKRD1 knock-down led to an enhancement of the relative expression level of biomarkers RUNX2, SP7 (Sp7 transcription factor), also known as osterix, and ALPL (Fig. 5c) at the transcriptional level. We further found that the enhanced accumulation of the matrix mineralization and the promoted ALPL enzyme activity supported the above-enhanced gene and protein expression (Fig. 5e, f). In all, our results indicated that ANKRD1 promoted adipogenesis and inhibited osteoblastogenesis.

IGF1 was significantly differentially up-regulated by 5.79, 4.73, and 4.92 folds during adipogenesis and down-regulated by 4.66, 5.41, and 13.75 folds during osteoblastogenesis (Fig. 2). For adipogenesis, IGF1 knockdown weakened the gene expression level of adipogenic and lipid droplet formation (Fig. 5c, d). Interestingly, IGF1 overexpression enforced gene

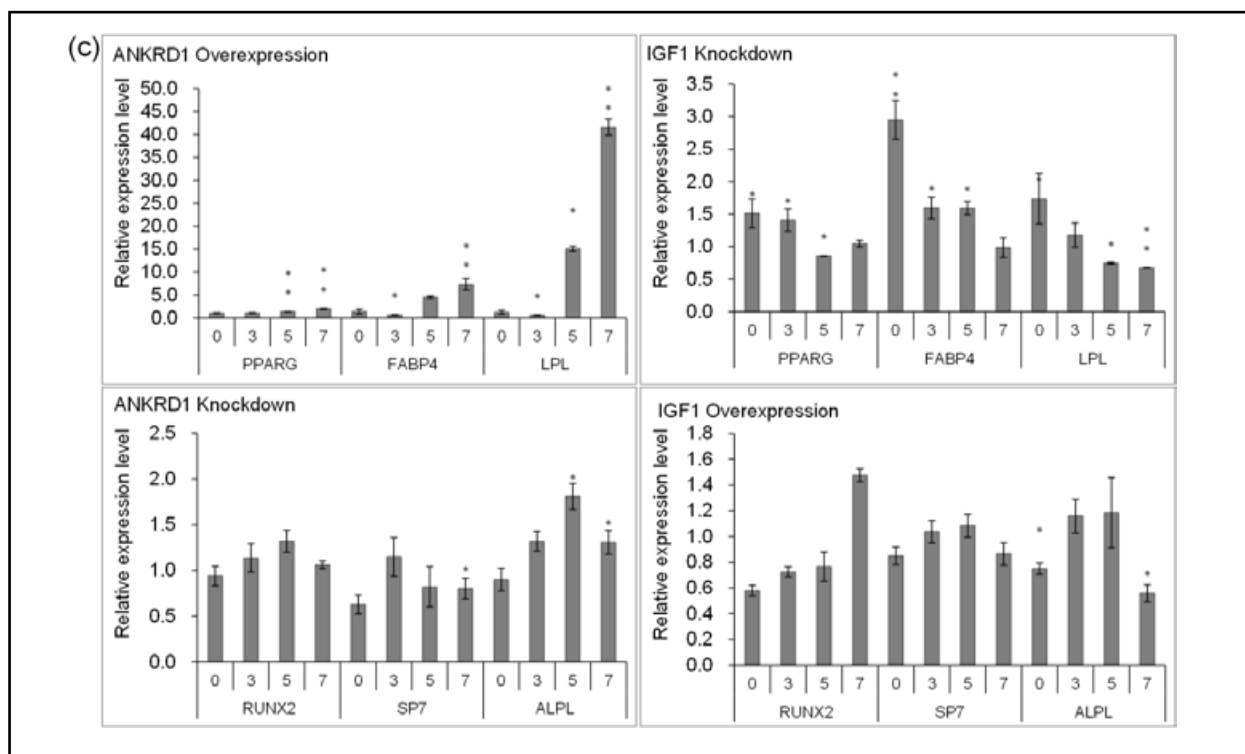
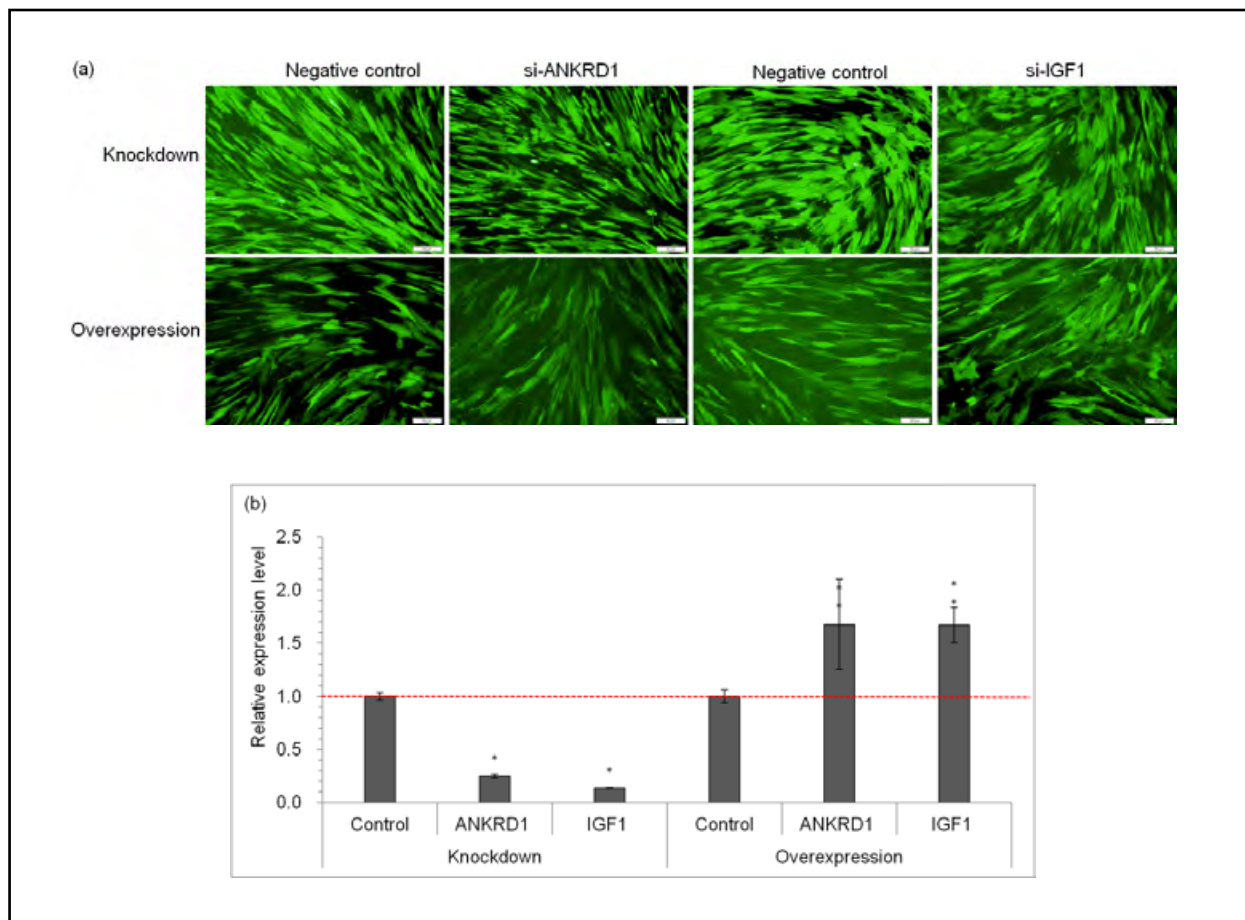


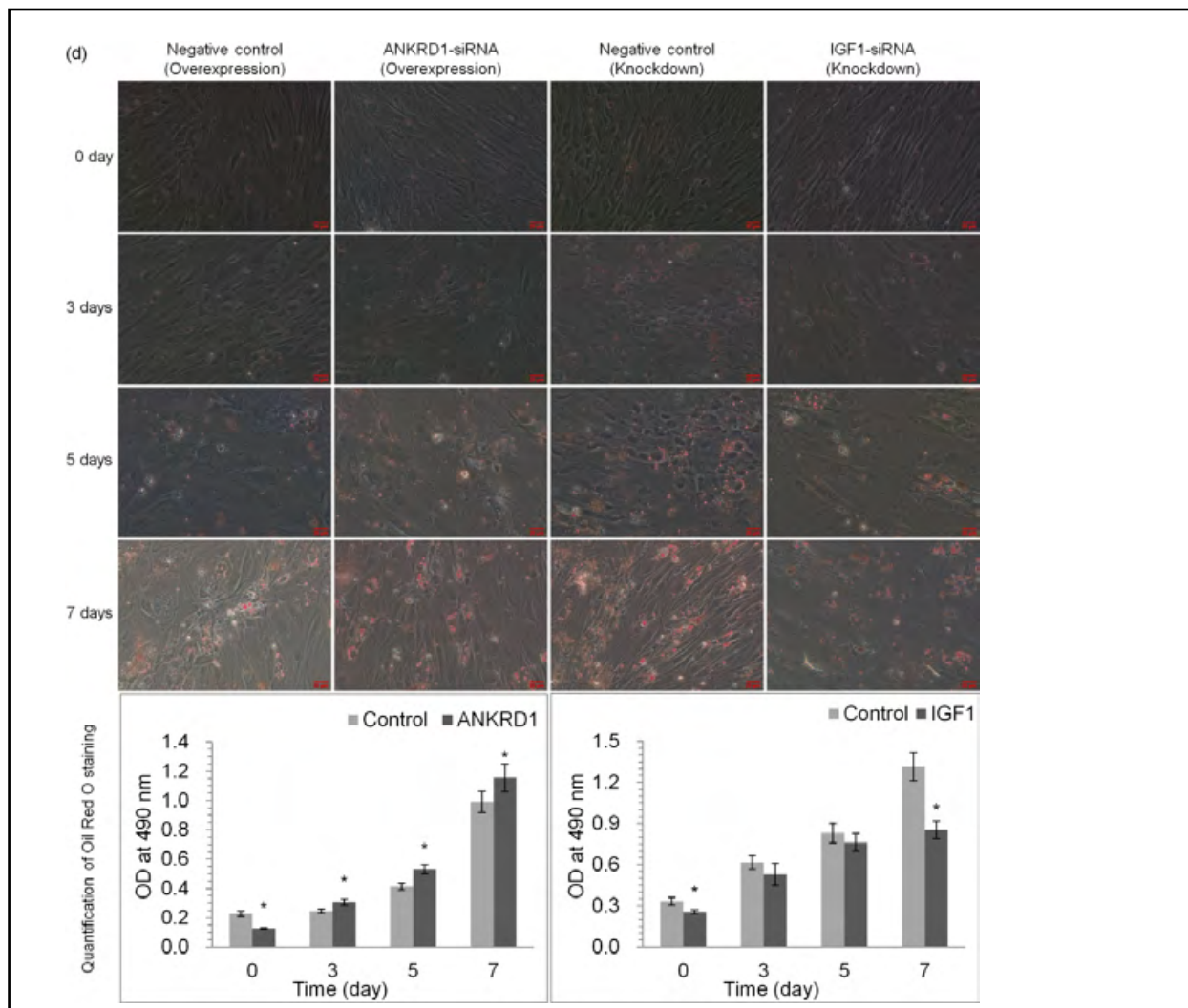


**Figure 3.** Gene ontogenesis (GO) analysis of the 275 DEGs shared by early adipo-osteoblastogenesis from hMSCs.



**Figure 4.** KEGG pathway analysis of the 275 DEGs shared by early adipo-osteoblastogenesis from hMSCs.





expression of biomarkers, the accumulation of the matrix mineralization, and ALPL enzyme activity during osteoblastogenesis (Fig. 5c, 5d, 5f). In conclusion, IGF1 was of anxo-action for adipo-osteoblastogenesis.

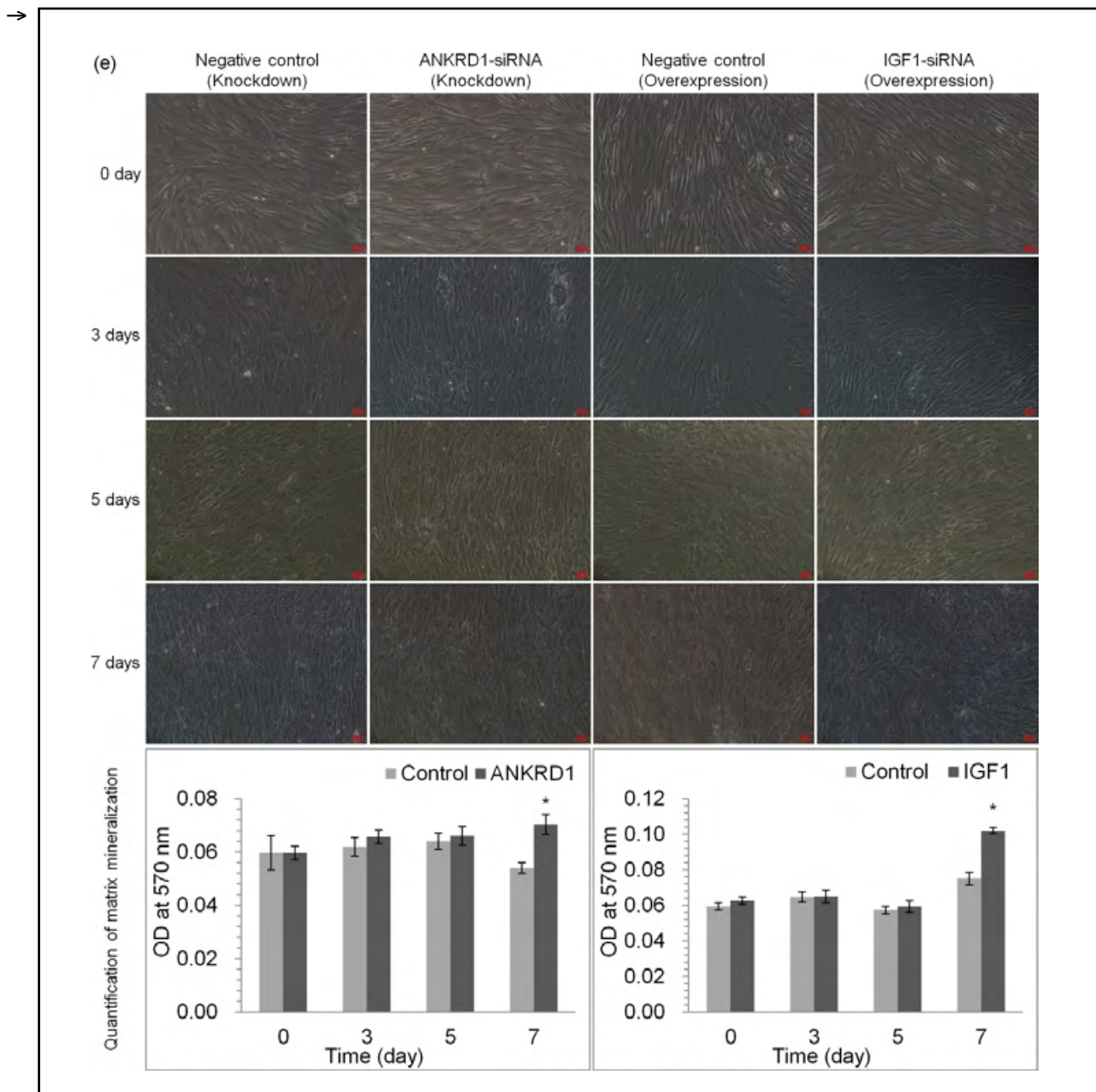
### Discussion

Upon receiving the proper signals, hMSCs, one multipotent progenitor, matured into adipo-osteogenic lineages, including adipocytes and osteoblastocytes [9, 33]. Here, our adipogenesis was markedly characterized by the gradually increasing lipid droplets from 3 to 7 days. Although the deposition of calcium in the extracellular matrix was less during osteoblastogenesis, it was also confirmed that the hMSCs differentiated along osteoblastogenesis for the rounded and cobblestone-like cell shape property and ALPL secretion.

In our study, the predominant gene repression was one of the molecular mechanisms for the com-

mitted pre-adipocyte and osteo-progenitor during early adipo-osteoblastogenesis, and thus agreed with the documented study [20]. However, gene expression was generally up-regulated in both mature cell lineages during late adipo-osteoblastogenesis [20, 34]. Our previous study supported PI3K-Akt signaling pathway closely correlated with adipogenesis at 7, 14, 21, and 28 days [35]. And the growing evidence also agreed with osteoblastogenesis largely depending on PI3K-Akt signaling pathway [36, 37]. In brief, although adipo-osteoblastogenesis were two different differentiation events, they also simultaneously shared the candidate genes.

ANKRD1 encoding ankyrin repeat domain 1 also known as CARP (cardiac ankyrin repeat protein), a transcriptional factor, was highly expressed in the heart and muscle tissue and mediates TGF- $\beta$  signaling in response to injury and stress [38–40]. For ANKRD1, the participation in adipogenesis [41] and the regulation by YAP/TAZ (Yes-associated protein/



/transcriptional coactivator with PDZ-binding motif) in osteoblastogenesis from dental pulp stem cells (DP-SCs) [42, 43] agreed with our gene function validation.

Similar to insulin in function and structure, *IGF1* encoding insulin-like growth factor 1 was involved in mediating growth and development. Our results were supported by the documented gene function of *IGF1* stimulating adipogenesis [44, 45] and promoting osteoblastogenesis [46, 47].

In summary, in this study, we elaborated a complete gene transcriptional picture of adipo-osteoblastogenesis from hMSCs using RNA-Seq technique. 275 DEGs were identified as candidate genes simulta-

neously shared by adipo-osteoblastogenesis, especially with the down-regulated gene most prevalent and the mostly enriched PI3K-AKT signaling pathway. Furthermore, *via* RNAi method, we further confirmed that ANKRD1 (ankyrin repeat domain 1) promoted adipogenesis and inhibited osteoblastogenesis, and IGF1 (insulin-like growth factor 1) simultaneously facilitated two differentiation events. Our understanding of adipo-osteoblastogenic process would provide candidate genes as molecular switches to control the adipocyte/osteoblastocyte balance or hMSCs fate choices and clues to screen the factors for the study and therapy of metabolic bone disease osteoporosis.

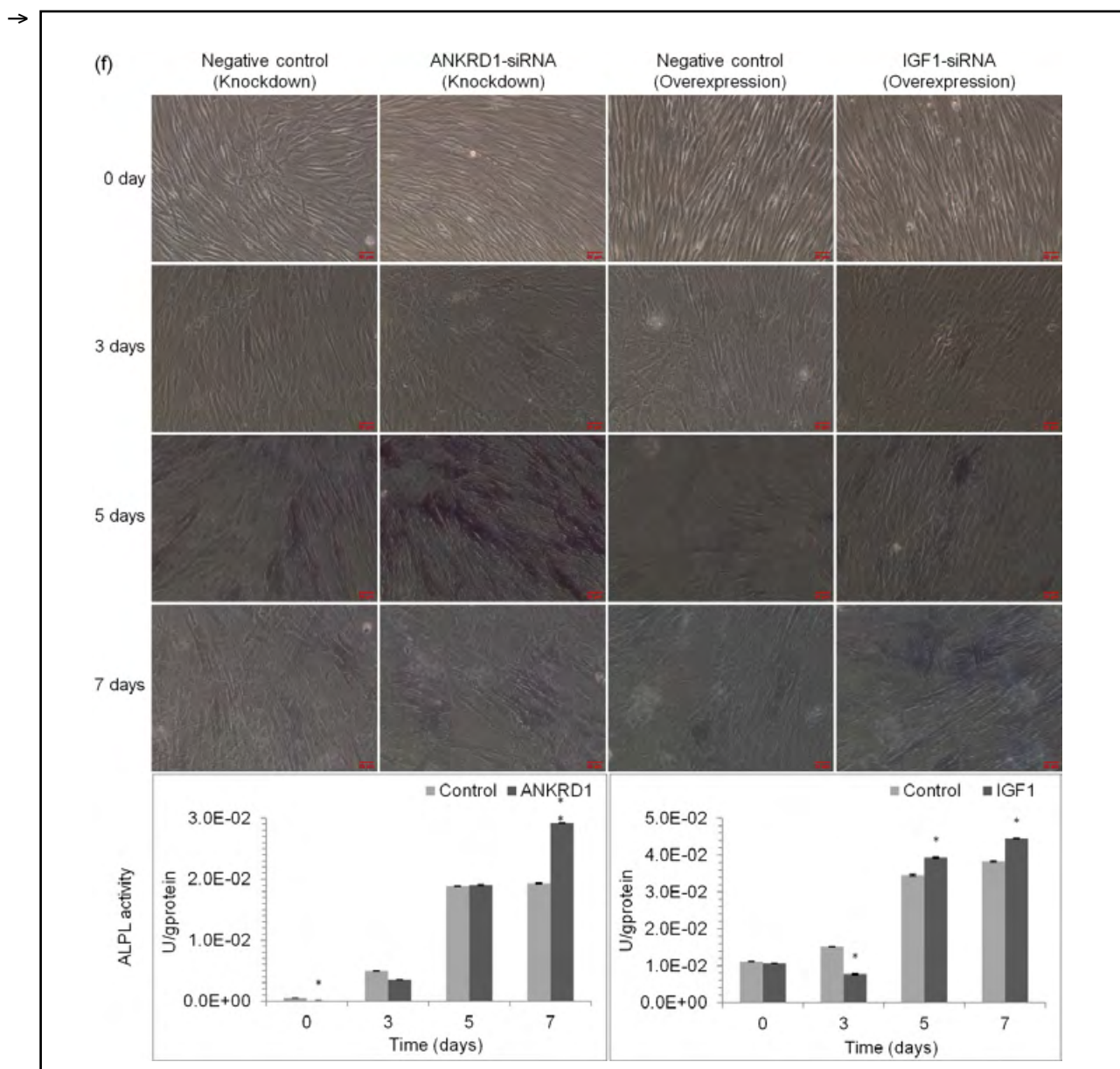


**Figure 5.** *ANKRD1* and *IGF1* regulate adipo-osteoblastogenesis from hMSCs; (a) Fluorescence intensity of *GFP* reporter gene after RNAi. Scale bar: 50  $\mu$ m; (b) The relative expression level of the candidate genes *ANKRD1* and *IGF1* after RNAi; (c) The relative expression level of the biomarkers, such as *FABP4*, *PPARG*, and *LPL* for adipogenesis and *RUNX2*, *SP7*, and *ALPL* for osteoblastogenesis; (d) Evaluation of adipogenic potential of hMSCs demonstrated by Oil Red O staining. Scale bar: 20  $\mu$ m; (e) Evaluation of osteoblastogenic potential by Alizarin Red staining. Scale bar: 20  $\mu$ m; (f) ALPL staining and enzyme activity. Scale bar: 20  $\mu$ m. Derived from Student's *t*-test (or the Mann-Whitney Rank Sum Test) wherever appropriate depending normality test, \* and \*\* separately indicate significant differences at  $p < 0.05$  and  $p < 0.001$ , respectively (SigmaPlot software, version 14, SPSS, USA).

## Funding

This research was supported by the National Natural Science Foundation of China (82160174/81860165) and Jiangxi Provincial Natural Science Foundation (20202ACB206003).

## Author contributions

XY designed the experiment, partially analyzed the RNA-Seq data and visualized data presentation, performed qRT-PCR experiment, and prepared the manuscript. XY, PW, YYF, YG, and JYL performed cell culture. XY, JJX, and XYX were in charge of the overall project. All authors read and approved the final manuscript.

## Ethics approval

With written informed consent signed, a 21-year-old non-osteoporotic healthy male volunteer was recruited by Affiliated Hospital of Jiujiang University in this study. The study is compliant with all relevant ethical regulations approved by the Medical Ethics Committee of Jiujiang University (Approved ID: 1-2013, February 20, 2013).

## Data availability statements

RNA-Seq sequence data were deposited in the GEO database at NCBI. The data can be accessed via reference number GSE174794.

## Conflict of interests

The authors declare that there are no competing interests associated with the manuscript.

## References

- Pittenger MF, Mackay AM, Beck SC, et al. Multilineage potential of adult human mesenchymal stem cells. *Science*. 1999; 284(5411): 143–147, doi: [10.1126/science.284.5411.143](https://doi.org/10.1126/science.284.5411.143), indexed in Pubmed: [10102814](https://pubmed.ncbi.nlm.nih.gov/10102814/).
- Giordano A, Cesari P, Capparuccia L, et al. Sema3A and neuropilin-1 expression and distribution in rat white adipose tissue. *Journal of Neurocytology*. 2003; 32(4): 345–352, doi: [10.1023/b:neur.0000011328.61376.bb](https://doi.org/10.1023/b:neur.0000011328.61376.bb).
- Nuttall ME, Gimble JM. Controlling the balance between osteoblastogenesis and adipogenesis and the consequent therapeutic implications. *Curr Opin Pharmacol*. 2004; 4(3): 290–294, doi: [10.1016/j.coph.2004.03.002](https://doi.org/10.1016/j.coph.2004.03.002), indexed in Pubmed: [15140422](https://pubmed.ncbi.nlm.nih.gov/15140422/).
- Liu Z, Liu H, He J, et al. Myeloma cells shift osteoblastogenesis to adipogenesis by inhibiting the ubiquitin ligase MURF1 in mesenchymal stem cells. *Sci Signal*. 2020; 13(633): eaay8203, doi: [10.1126/scisignal.aay8203](https://doi.org/10.1126/scisignal.aay8203), indexed in Pubmed: [32457115](https://pubmed.ncbi.nlm.nih.gov/32457115/).
- Fan J, Lee CS, Kim S, et al. Trb3 controls mesenchymal stem cell lineage fate and enhances bone regeneration by scaffold-mediated local gene delivery. *Biomaterials*. 2021; 264: 120445, doi: [10.1016/j.biomaterials.2020.120445](https://doi.org/10.1016/j.biomaterials.2020.120445), indexed in Pubmed: [33069136](https://pubmed.ncbi.nlm.nih.gov/33069136/).
- Li H, Fan J, Fan L, et al. MiRNA-10b reciprocally stimulates osteogenesis and inhibits adipogenesis partly through the tgf- / smad2 signaling pathway. *Aging Dis*. 2018; 9(6): 1058–1073, doi: [10.14336/AD.2018.0214](https://doi.org/10.14336/AD.2018.0214), indexed in Pubmed: [30574418](https://pubmed.ncbi.nlm.nih.gov/30574418/).
- Li R, Zhang W, Yan Z, et al. Long non-coding RNA (LncRNA) HOTAIR regulates BMP9-induced osteogenic differentiation by targeting the proliferation of mesenchymal stem cells (MSCs). *Aging (Albany NY)*. 2021; 13(3): 4199–4214, doi: [10.18632/aging.202384](https://doi.org/10.18632/aging.202384), indexed in Pubmed: [33461171](https://pubmed.ncbi.nlm.nih.gov/33461171/).
- Ji H, Cui Xu, Yang Y, et al. CircRNA hsa\_circ\_0006215 promotes osteogenic differentiation of BMSCs and enhances osteogenesis-angiogenesis coupling by competitively binding to miR-942-5p and regulating RUNX2 and VEGF. *Aging (Albany NY)*. 2021; 13(7): 10275–10288, doi: [10.18632/aging.202791](https://doi.org/10.18632/aging.202791), indexed in Pubmed: [33819188](https://pubmed.ncbi.nlm.nih.gov/33819188/).
- Frith J, Genever P. Transcriptional control of mesenchymal stem cell differentiation. *Transfus Med Hemother*. 2008; 35(3): 216–227, doi: [10.1159/000127448s](https://doi.org/10.1159/000127448s), indexed in Pubmed: [21547119](https://pubmed.ncbi.nlm.nih.gov/21547119/).
- Komori T. Regulation of osteoblast differentiation by transcription factors. *J Cell Biochem*. 2006; 99(5): 1233–1239, doi: [10.1002/jcb.20958](https://doi.org/10.1002/jcb.20958), indexed in Pubmed: [16795049](https://pubmed.ncbi.nlm.nih.gov/16795049/).
- Hong JH, Hwang ES, McManus MT, et al. TAZ, a transcriptional modulator of mesenchymal stem cell differentiation. *Science*. 2005; 309(5737): 1074–1078, doi: [10.1126/science.1110955](https://doi.org/10.1126/science.1110955), indexed in Pubmed: [16099986](https://pubmed.ncbi.nlm.nih.gov/16099986/).
- Shen J, James AW, Zhang X, et al. Novel wnt regulator NEL-like molecule-1 antagonizes adipogenesis and augments osteogenesis induced by bone morphogenetic protein 2. *Am J Pathol*. 2016; 186(2): 419–434, doi: [10.1016/j.ajpath.2015.10.011](https://doi.org/10.1016/j.ajpath.2015.10.011), indexed in Pubmed: [26772960](https://pubmed.ncbi.nlm.nih.gov/26772960/).
- Takada I, Kouzmenko AP, Kato S. Wnt and PPARgamma signaling in osteoblastogenesis and adipogenesis. *Nat Rev Rheumatol*. 2009; 5(8): 442–447, doi: [10.1038/nrrheum.2009.137](https://doi.org/10.1038/nrrheum.2009.137), indexed in Pubmed: [19581903](https://pubmed.ncbi.nlm.nih.gov/19581903/).
- Choi HK, Yuan H, Fang F, et al. Tsc1 regulates the balance between osteoblast and adipocyte differentiation through autophagy/notch1/ $\beta$ -catenin cascade. *J Bone Miner Res*. 2018; 33(11): 2021–2034, doi: [10.1002/jbmr.3530](https://doi.org/10.1002/jbmr.3530), indexed in Pubmed: [29924882](https://pubmed.ncbi.nlm.nih.gov/29924882/).
- Park JS, Kim M, Song NJ, et al. A reciprocal role of the smad4-taz axis in osteogenesis and adipogenesis of mesenchymal stem cells. *Stem Cells*. 2019; 37(3): 368–381, doi: [10.1002/stem.2949](https://doi.org/10.1002/stem.2949), indexed in Pubmed: [30444564](https://pubmed.ncbi.nlm.nih.gov/30444564/).
- Muruganandan S, Govindarajan R, McMullen NM, et al. Chemokine-Like receptor 1 is a novel wnt target gene that regulates mesenchymal stem cell differentiation. *Stem Cells*. 2017; 35(3): 711–724, doi: [10.1002/stem.2520](https://doi.org/10.1002/stem.2520), indexed in Pubmed: [27733019](https://pubmed.ncbi.nlm.nih.gov/27733019/).
- Zhang C, Li L, Jiang Y, et al. Space microgravity drives trans-differentiation of human bone marrow-derived mesenchymal stem cells from osteogenesis to adipogenesis. *FASEB J*. 2018; 32(8): 4444–4458, doi: [10.1096/fj.201700208RR](https://doi.org/10.1096/fj.201700208RR), indexed in Pubmed: [29533735](https://pubmed.ncbi.nlm.nih.gov/29533735/).
- Yang S, Guo L, Su Y, et al. Nitric oxide balances osteoblast and adipocyte lineage differentiation via the JNK/MAPK signaling pathway in periodontal ligament stem cells. *Stem Cell Res Ther*. 2018; 9(1): 118, doi: [10.1186/s13287-018-0869-2](https://doi.org/10.1186/s13287-018-0869-2), indexed in Pubmed: [29716662](https://pubmed.ncbi.nlm.nih.gov/29716662/).
- Han P, Frith JE, Gomez GA, et al. Five piconewtons: the difference between osteogenic and adipogenic fate choice in human mesenchymal stem cells. *ACS Nano*. 2019; 13(10): 11129–11143, doi: [10.1021/acs.nano.9b03914](https://doi.org/10.1021/acs.nano.9b03914), indexed in Pubmed: [31580055](https://pubmed.ncbi.nlm.nih.gov/31580055/).
- Scheideler M, Elabd C, Zaragosi LE, et al. Comparative transcriptomics of human multipotent stem cells during adipogenesis and osteoblastogenesis. *BMC Genomics*. 2008; 9: 340, doi: [10.1186/1471-2164-9-340](https://doi.org/10.1186/1471-2164-9-340), indexed in Pubmed: [18637193](https://pubmed.ncbi.nlm.nih.gov/18637193/).
- Li L, Zhang C, Chen JL, et al. Effects of simulated microgravity on the expression profiles of RNA during osteogenic differentiation of human bone marrow mesenchymal stem cells. *Cell Prolif*. 2019; 52(2): e12539, doi: [10.1111/cpr.12539](https://doi.org/10.1111/cpr.12539), indexed in Pubmed: [30397970](https://pubmed.ncbi.nlm.nih.gov/30397970/).
- Bai M, Han Y, Wu Y, et al. Targeted genetic screening in mice through haploid embryonic stem cells identifies critical genes in bone development. *PLoS Biol*. 2019; 17(7): e3000350, doi: [10.1371/journal.pbio.3000350](https://doi.org/10.1371/journal.pbio.3000350), indexed in Pubmed: [31265461](https://pubmed.ncbi.nlm.nih.gov/31265461/).
- Xu X, Li X, Yan R, et al. Gene expression profiling of human bone marrow-derived mesenchymal stem cells during adipogenesis. *Folia Histochem Cytobiol*. 2016; 54(1): 14–24, doi: [10.5603/FHC.a2016.0003](https://doi.org/10.5603/FHC.a2016.0003), indexed in Pubmed: [27044590](https://pubmed.ncbi.nlm.nih.gov/27044590/).

24. Casado-Díaz A, Anter J, Müller S, et al. Transcriptomic analyses of adipocyte differentiation from human mesenchymal stromal-cells (MSC). *J Cell Physiol.* 2017; 232(4): 771–784, doi: [10.1002/jcp.25472](https://doi.org/10.1002/jcp.25472), indexed in Pubmed: [27349923](https://pubmed.ncbi.nlm.nih.gov/27349923/).
25. Yi X, Liu J, Wu P, et al. The key microRNA on lipid droplet formation during adipogenesis from human mesenchymal stem cells. *J Cell Physiol.* 2020; 235(1): 328–338, doi: [10.1002/jcp.28972](https://doi.org/10.1002/jcp.28972), indexed in Pubmed: [31210354](https://pubmed.ncbi.nlm.nih.gov/31210354/).
26. Nakamura T, Shiojima S, Hirai Y, et al. Temporal gene expression changes during adipogenesis in human mesenchymal stem cells. *Biochemical and Biophysical Research Communications.* 2003; 303(1): 306–312, doi: [10.1016/s0006-291x\(03\)00325-5](https://doi.org/10.1016/s0006-291x(03)00325-5).
27. Ross SE, Hemati N, Longo KA, et al. Inhibition of adipogenesis by Wnt signaling. *Science.* 2000; 289(5481): 950–953, doi: [10.1126/science.289.5481.950](https://doi.org/10.1126/science.289.5481.950), indexed in Pubmed: [10937998](https://pubmed.ncbi.nlm.nih.gov/10937998/).
28. Donzelli E, Lucchini C, Ballarini E, et al. ERK1 and ERK2 are involved in recruitment and maturation of human mesenchymal stem cells induced to adipogenic differentiation. *J Mol Cell Biol.* 2011; 3(2): 123–131, doi: [10.1093/jmcb/mjq050](https://doi.org/10.1093/jmcb/mjq050), indexed in Pubmed: [21278199](https://pubmed.ncbi.nlm.nih.gov/21278199/).
29. Chen J, Liu M, Luo X, et al. Exosomal miRNA-486-5p derived from rheumatoid arthritis fibroblast-like synoviocytes induces osteoblast differentiation through the Tob1/BMP/Smad pathway. *Biomater Sci.* 2020; 8(12): 3430–3442, doi: [10.1039/c9bm01761e](https://doi.org/10.1039/c9bm01761e), indexed in Pubmed: [32406432](https://pubmed.ncbi.nlm.nih.gov/32406432/).
30. Zou D, Han W, You S, et al. In vitro study of enhanced osteogenesis induced by HIF-1 $\alpha$ -transduced bone marrow stem cells. *Cell Prolif.* 2011; 44(3): 234–243, doi: [10.1111/j.1365-2184.2011.00747.x](https://doi.org/10.1111/j.1365-2184.2011.00747.x), indexed in Pubmed: [21535264](https://pubmed.ncbi.nlm.nih.gov/21535264/).
31. Anders S, Pyl PT, Huber W. HTSeq—a Python framework to work with high-throughput sequencing data. *Bioinformatics.* 2015; 31(2): 166–169, doi: [10.1093/bioinformatics/btu638](https://doi.org/10.1093/bioinformatics/btu638), indexed in Pubmed: [25260700](https://pubmed.ncbi.nlm.nih.gov/25260700/).
32. Livak KJ, Schmittgen TD. Analysis of relative gene expression data using real-time quantitative PCR and the 2<sup>(-Delta Delta C(T))</sup> Method. *Methods.* 2001; 25(4): 402–408, doi: [10.1006/meth.2001.1262](https://doi.org/10.1006/meth.2001.1262), indexed in Pubmed: [11846609](https://pubmed.ncbi.nlm.nih.gov/11846609/).
33. Augello A, Kurth TB, De Bari C. Mesenchymal stem cells: a perspective from in vitro cultures to in vivo migration and niches. *Eur Cell Mater.* 2010; 20: 121–133, doi: [10.22203/ecm.v020a11](https://doi.org/10.22203/ecm.v020a11), indexed in Pubmed: [21249629](https://pubmed.ncbi.nlm.nih.gov/21249629/).
34. Yi X, Wu P, Liu J, et al. Identification of the potential key genes for adipogenesis from human mesenchymal stem cells by RNA-Seq. *J Cell Physiol.* 2019; 234(11): 20217–20227, doi: [10.1002/jcp.28621](https://doi.org/10.1002/jcp.28621), indexed in Pubmed: [30989650](https://pubmed.ncbi.nlm.nih.gov/30989650/).
35. Yi X, Liu J, Wu P, et al. The whole transcriptional profiling of cellular metabolism during adipogenesis from hMSCs. *J Cell Physiol.* 2020; 235(1): 349–363, doi: [10.1002/jcp.28974](https://doi.org/10.1002/jcp.28974), indexed in Pubmed: [31237701](https://pubmed.ncbi.nlm.nih.gov/31237701/).
36. Ma P, Gu B, Ma J, et al. Glimepiride induces proliferation and differentiation of rat osteoblasts via the PI3-kinase/Akt pathway. *Metabolism.* 2010; 59(3): 359–366, doi: [10.1016/j.metabol.2009.08.003](https://doi.org/10.1016/j.metabol.2009.08.003), indexed in Pubmed: [19800638](https://pubmed.ncbi.nlm.nih.gov/19800638/).
37. Yan X, Wu H, Wu Z, et al. The new synthetic HS-releasing SDSS protects MC3T3-E1 osteoblasts against HO-induced apoptosis by suppressing oxidative stress, inhibiting MAPKs, and activating the PI3K/Akt pathway. *Front Pharmacol.* 2017; 8: 07, doi: [10.3389/fphar.2017.00007](https://doi.org/10.3389/fphar.2017.00007), indexed in Pubmed: [28163684](https://pubmed.ncbi.nlm.nih.gov/28163684/).
38. Bogomolovas J, Brohm K, Čelutkienė J, et al. Induction of ankrd1 in dilated cardiomyopathy correlates with the heart failure progression. *Biomed Res Int.* 2015; 2015: 273936, doi: [10.1155/2015/273936](https://doi.org/10.1155/2015/273936), indexed in Pubmed: [25961010](https://pubmed.ncbi.nlm.nih.gov/25961010/).
39. Samaras SE, Almodóvar-García K, Wu N, et al. Global deletion of Ankrd1 results in a wound-healing phenotype associated with dermal fibroblast dysfunction. *Am J Pathol.* 2015; 185(1): 96–109, doi: [10.1016/j.ajpath.2014.09.018](https://doi.org/10.1016/j.ajpath.2014.09.018), indexed in Pubmed: [25452119](https://pubmed.ncbi.nlm.nih.gov/25452119/).
40. Almodóvar-García K, Kwon M, Samaras SE, et al. ANKRD1 acts as a transcriptional repressor of MMP13 via the AP-1 site. *Mol Cell Biol.* 2014; 34(8): 1500–1511, doi: [10.1128/MCB.01357-13](https://doi.org/10.1128/MCB.01357-13), indexed in Pubmed: [24515436](https://pubmed.ncbi.nlm.nih.gov/24515436/).
41. Zhang Q, Lee HG, Han JA, et al. Differentially expressed proteins associated with myogenesis and adipogenesis in skeletal muscle and adipose tissue between bulls and steers. *Mol Biol Rep.* 2012; 39(2): 953–960, doi: [10.1007/s11033-011-0821-3](https://doi.org/10.1007/s11033-011-0821-3), indexed in Pubmed: [21594731](https://pubmed.ncbi.nlm.nih.gov/21594731/).
42. Lee E, Ko JY, Kim J, et al. Osteogenesis and angiogenesis are simultaneously enhanced in BMP2-/VEGF-transfected adipose stem cells through activation of the YAP/TAZ signaling pathway. *Biomater Sci.* 2019; 7(11): 4588–4602, doi: [10.1039/c9bm01037h](https://doi.org/10.1039/c9bm01037h), indexed in Pubmed: [31435635](https://pubmed.ncbi.nlm.nih.gov/31435635/).
43. Zheng L, Zhang L, Chen L, et al. Static magnetic field regulates proliferation, migration, differentiation, and YAP/TAZ activation of human dental pulp stem cells. *J Tissue Eng Regen Med.* 2018; 12(10): 2029–2040, doi: [10.1002/term.2737](https://doi.org/10.1002/term.2737), indexed in Pubmed: [30058115](https://pubmed.ncbi.nlm.nih.gov/30058115/).
44. Scavo LM, Karas M, Murray M, et al. Insulin-like growth factor-I stimulates both cell growth and lipogenesis during differentiation of human mesenchymal stem cells into adipocytes. *J Clin Endocrinol Metab.* 2004; 89(7): 3543–3553, doi: [10.1210/jc.2003-031682](https://doi.org/10.1210/jc.2003-031682), indexed in Pubmed: [15240644](https://pubmed.ncbi.nlm.nih.gov/15240644/).
45. Hu Li, Yang G, Hägg D, et al. IGF1 promotes adipogenesis by a lineage bias of endogenous adipose stem/progenitor cells. *Stem Cells.* 2015; 33(8): 2483–2495, doi: [10.1002/stem.2052](https://doi.org/10.1002/stem.2052), indexed in Pubmed: [26010009](https://pubmed.ncbi.nlm.nih.gov/26010009/).
46. Xue P, Wu X, Zhou L, et al. IGF1 promotes osteogenic differentiation of mesenchymal stem cells derived from rat bone marrow by increasing TAZ expression. *Biochem Biophys Res Commun.* 2013; 433(2): 226–231, doi: [10.1016/j.bbrc.2013.02.088](https://doi.org/10.1016/j.bbrc.2013.02.088), indexed in Pubmed: [23473758](https://pubmed.ncbi.nlm.nih.gov/23473758/).
47. Zeng Q, Wang Y, Gao J, et al. miR-29b-3p regulated osteoblast differentiation via regulating IGF-1 secretion of mechanically stimulated osteocytes. *Cell Mol Biol Lett.* 2019; 24: 11, doi: [10.1186/s11658-019-0136-2](https://doi.org/10.1186/s11658-019-0136-2), indexed in Pubmed: [30915127](https://pubmed.ncbi.nlm.nih.gov/30915127/).

*Submitted: 19 March, 2022*

*Accepted after reviews: 5 May, 2022*

*Available as AoP: 16 May, 2022*